Complexation with diol host compounds. Part 24.† Kinetics of desolvation of inclusion compounds of 2,7-substituted 2,2′-bis(9-hydroxy-9-fluorenyl)biphenyl hosts with acetone

Mino R. Caira,[a] Anita Coetzee,*[,a] Luigi R. Nassimbeni,[a] Edwin Weber[b] and Andreas Wierig[b]

[a] *Department of Chemistry, University of Cape Town, Rondebosch 7700, South Africa*
[b] *Institut für Organische Chemie, Technische Universität Bergakademie Freiberg, Leipziger Strasse 29, D-09596 Freiberg, Germany*

The structures of the acetone inclusion compounds of 2,2′-bis(2,7-dichloro-9-hydroxy-9-fluorenyl)-biphenyl (compound 1) and 2,2′-bis(2,7-di-*tert*-butyl-9-hydroxy-9-fluorenyl)biphenyl (compound 2), with host : guest ratios of 1 : 2 and 1 : 1, respectively, have been elucidated. Compound 2 desolvates at 175 °C, whereas compound 1 is much less stable and desolvates at 80 °C. Compound 1 desolvates in a single deceleratory step following a three dimensional diffusion kinetic model. The desolvation of compound 2 follows the first-order kinetic model. The activation energies of desolvation have been evaluated.

Introduction

Organic molecules that form crystalline host–guest inclusion compounds have been studied extensively.[2,3] Host molecules including the hydroxy moiety have proved to be very successful and form inclusion compounds with a wide variety of guests.[4–6] Often hydrogen bonding between the host and guest gives rise to remarkably stable inclusion compounds.[7,8] In view of the practical uses of inclusion compounds, *e.g.* in chemical separation and stabilisation,[9] their reactivity and stability are of interest. Yet, very little attention has been paid to the thermal decomposition of organic inclusion compounds. This may be due to the fact that the decomposition often involves multiple steps, with the formation of new intermediate host–guest phases, whose composition and structure are not readily established. We have recently investigated the kinetics of desolvation of the benzene inclusion compounds of two related substituted *trans*-9,10-dihydroxy-9,10-dihydroanthracenes.[10] We have also studied the thermal desolvation of the inclusion compounds of 2,2′-bis(2,7-dichloro-9-hydroxy-9-fluorenyl)biphenyl with 1,4-dioxane and 1,3-dioxolane.[11] The kinetics were analysed by isothermal thermogravimetry (TG) at selected temperatures, and curve fitting techniques allowed us to select suitable models to describe the desolvation mechanism and derive the appropriate Arrhenius parameters.

We now present the results of the structures and thermal desolvation of the acetone inclusion compounds of two related hosts, 2,2′-bis(2,7-dichloro-9-hydroxy-9-fluorenyl)biphenyl (compound **1**) and 2,2′-bis(2,7-di-*tert*-butyl-9-hydroxy-9-fluorenyl)biphenyl (compound **2**).

Experimental

The inclusion compounds were formed by dissolving the appropriate host compounds[8] in an excess of acetone. Crystals of diffraction quality were obtained by slow evaporation of the solutions. X-Ray diffraction data were measured on an Enraf-Nonius CAD4 diffractometer, using graphite-monochromated radiation, (λ = 0.7107 Å) and the ω-2θ scan mode. The selected crystals were sealed in Lindemann capillary tubes together with mother liquor in order to prevent desorption of the guest. During data collection three reference reflections were monitored periodically to check crystal stability. The data reduction included correction for Lorentz and polarisation effects and an absorption correction in the case of compound **1**. Crystal data and structural refinement parameters are given in Table 1.‡

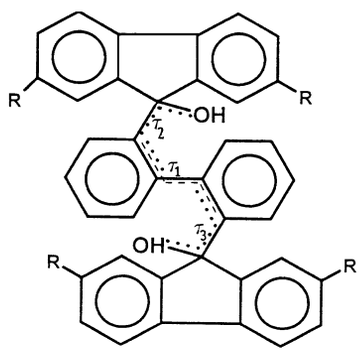

1 R = Cl

2 R = *tert*-butyl

Differential scanning calorimetry (DSC) and thermal gravimetry (TG) were performed on a Perkin-Elmer PC7 series system. Fine powdered specimens, obtained from continuously stirred solutions, were blotted dry on filter paper and placed in open platinum pans for TG experiments and in crimped but vented aluminium sample pans for DSC experiments. Sample weight in each case was 2–5 mg. The temperature range was typically 30–350 °C, at a heating rate of 20 °C min^{-1}. The samples were purged by a stream of nitrogen flowing at 40 ml min^{-1}. Data for the kinetics of desolvation were obtained from isothermal TG experiments done at selected temperatures in the range 40–65 °C for compound **1** and 125–145 °C for compound **2**.

X-Ray powder diffraction (XRD) patterns were recorded on a Philips PW1050/80 verticle goniometer with a PW1394 motor control unit. The powder patterns were collected over a 2θ range of 6–40°, at 0.1° 2θ intervals and 1s counts. Automatic receiving and divergence slits were used.

Infrared spectroscopy was carried out on a Perkin-Elmer 983 IR spectrometer. The samples were prepared in Nujol mulls,

† For Part 23, see ref. 1.

‡ Atomic co-ordinates, thermal parameters and bond lengths and angles have been deposited at the Cambridge Crystallographic Data Centre (CCDC). See 'Instructions for Authors', *J. Chem. Soc., Perkin Trans. 2*, 1997, Issue 1. Any request to the CCDC for this material should quote the full literature citation and the reference number 188/49.

Table 1 Crystal data and refinement parameters

Compound	**1**	**2**
Molecular formula	$C_{38}H_{22}O_2Cl_4 \cdot 2(C_3H_6O)$	$C_{54}H_{58}O_2 \cdot C_3H_6O$
M_r/g mol^{-1}	768.56	797.08
T/K	293(2)	294(2)
Crystal data		
Crystal system	Monoclinic	Monoclinic
Space group	*C*2/*c*	*C*2/*c*
a/Å	20.424(6)	17.120(2)
b/Å	11.496(3)	17.935(2)
c/Å	18.885(7)	17.232(3)
β/°	122.23(3)	114.15(1)
Z	4	4
V/Å^3	3751(2)	4828(1)
D_c/g cm^{-3}	1.322	1.097
μ(Mo-Kα)/cm^{-1}	3.59	0.66
F(000)	1592	1720
Data collection		
Crystal dimensions/mm	0.40 × 0.50 × 0.40	0.45 × 0.45 × 0.50
Range scanned *θ*/°	2.13–24.97	1.73–24.97
Range of indices *h*,*k*,*l*	−24, 20; 0, 13; 0, 22	−20, 18; 0, 21; 0, 20
No. of reflections collected	3397	4407
No. of unique reflections	3295	4252
No. of reflections observed with $I_{rel} > 2\sigma(I_{rel})$	1967	2200
Final refinement		
No. of restraints	2	4
No. of parameters	234	287
$R1$ ($I_{rel} > 2\sigma(I_{rel})$)	0.0643	0.0659
$wR2$ ($I_{rel} > 2\sigma(I_{rel})$)	0.1777	0.1802
Extinction coefficient	—	0.0034(5)
Max. height in electron density map/e Å^{-3}	0.631	0.510
Min. height in electron density map/e Å^{-3}	−0.462	−0.226
Absorption correction factor	0.9512–0.9980	—

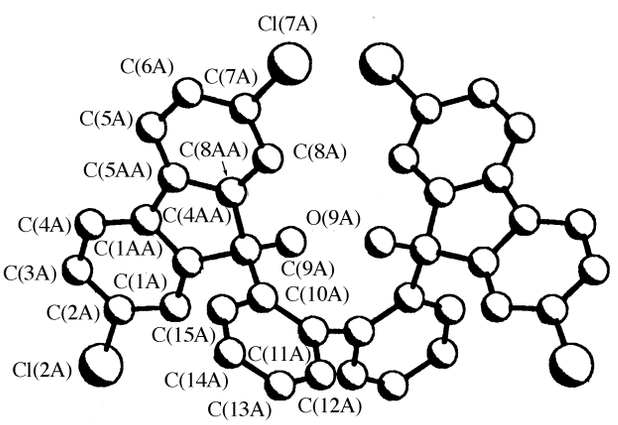

Fig. 1 The host in compound **1**, showing the numbering scheme

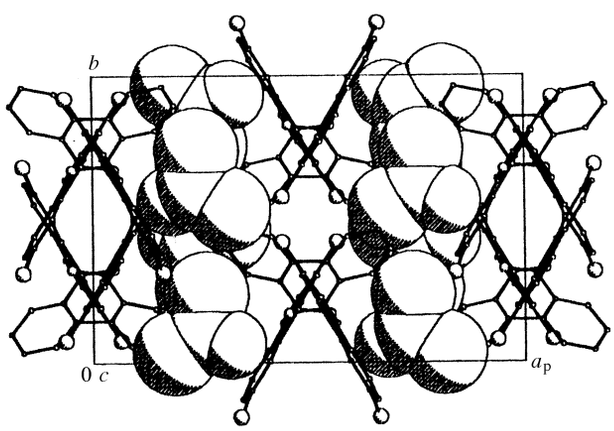

Fig. 2 The crystal packing in compound **1** as viewed down [001]. The guest molecules are represented with van der Waals radii.

with NaCl windows. The spectra were recorded over the range 4000–1000 cm^{-1}.

Results and discussion

Structure solution and refinement

The structures were solved by direct methods using SHELX-86[12] and refined by full-matrix least-squares methods on F^2, with SHELXL.[13] The systematic absences observed indicated that the space group was *Cc* or *C*2/*c*, in each case. The intensity statistics, obtained from direct methods, in each case indicated that the space groups were centrosymmetric, hence the space group *C*2/*c* was chosen. Direct methods yielded all the host non-hydrogen atoms in the asymmetric unit. The non-hydrogen atoms in the guest molecules were located in difference electron density maps upon subsequent refinement. In each case the hydroxy hydrogen atoms were located in difference electron density maps and refined with bond length constraints[14] and individual isotropic temperature factors. The rest of the host hydrogen atoms were placed with geometric constraints and refined with a common isotropic temperature factor. The guest hydrogen atoms were omitted from the final models. In the final refinement of compound **2** an extinction correction was applied, where F_c is multiplied by $k[1 + 0.001xF_c^2\lambda^3/\sin(2\theta)]^{-1/4}$ and x was refined by least-squares to a value of 0.0034(5). The weighting scheme used was $w = q/[\sigma^2(F_o^2) + (aP)^2 + (bP)]$, where a and b were defined for each structure and $P = [0.333\,33 \times \text{max. of } (0 \text{ or } F_o^2) + (1 - 0.333\,33)F_c^2]$.

For compound **1**, TG yielded a host : guest ratio of 1 : 2, and since it crystallises in the space group *C*2/*c* with $Z = 4$, this requires the host molecule to be in a special position, on the diad at Wyckoff position *e*. The structure of the host molecule with the atomic numbering scheme is shown in Fig. 1. The central biphenyl is twisted at right angles with the torsion angle C(10A)–C(11A)–C(11A′)–C(10A′) = 92.5(7)°. A projection of the structure viewed along [001] is shown in Fig. 2. The acetone

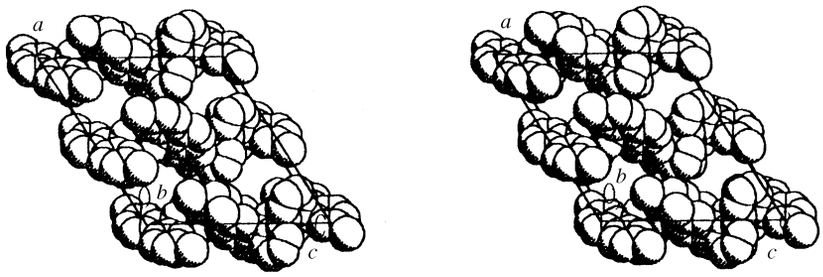

Fig. 3 Space filled diagram of the host network in compound **1** as viewed down [010]

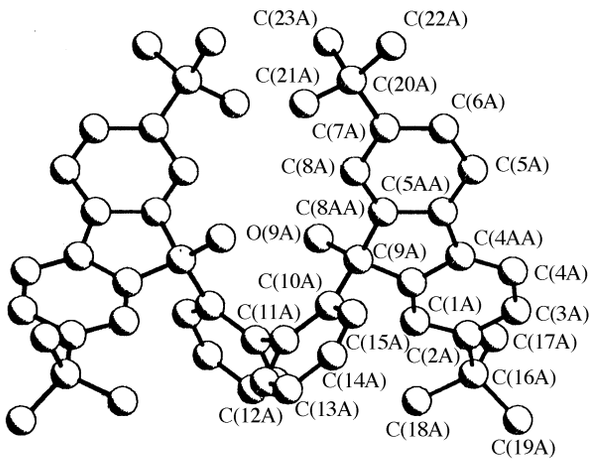

Fig. 4 The host in compound **2**, showing the numbering scheme

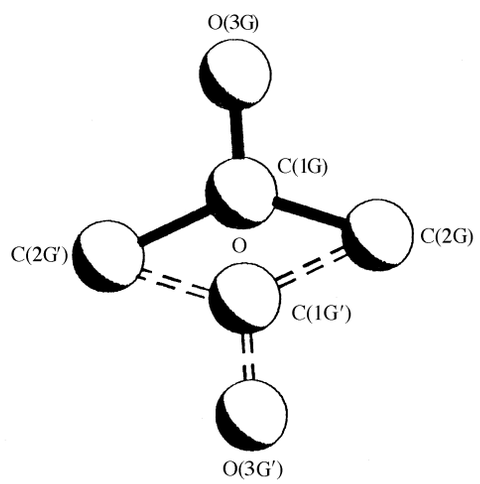

Fig. 5 Disorder in the acetone molecule, compound **2**

molecule was modelled with one of the methyl carbon atoms disordered over two positions, C(3GA) and C(3GB), each with a site occupancy of 0.5. The guest molecules are situated in channels running parallel to [010]. Fig. 3 shows a view down these channels, down [010]. The host molecules are represented with van der Waals radii and the guests were omitted for clarity. The structure is stabilised *via* a pair of equivalent hydrogen bonds O(9A)–H(9A)···O(1G), from the host hydroxy groups to the guest molecules [d(O···O) = 2.825(4) Å].

For compound **2**, which also crystallises in the space group $C2/c$ with $Z = 4$, a host : guest ratio of 1 : 1 was confirmed by TG. The host molecule is again located on a diad at Wyckoff position *e*. The conformation of the host molecule, with atomic numbering scheme, is shown in Fig. 4. The guest molecule is disordered over two positions, related by a centre of symmetry. The asymmetric unit consists of half a host molecule, and half of an acetone molecule, with O(3G) and C(1G) at a site occupancy of 0.5 each, and the methyl carbon C(2G) with full site occupancy, as shown in Fig. 5. A projection of the structure

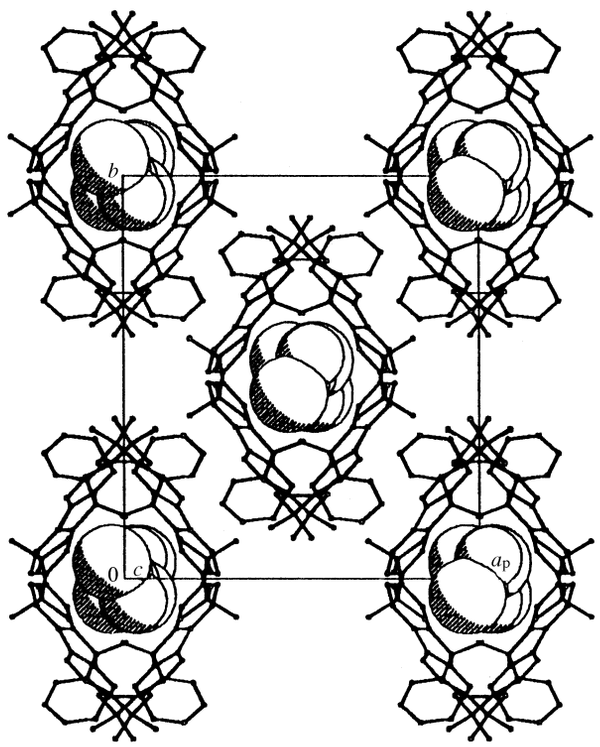

Fig. 6 The crystal packing in compound **2** as viewed down [001]. The guest molecules are represented with van der Waals radii.

Table 2 Selected torsion angles

Compound	R	Guest (H : G)	τ_1	τ_2	τ_3
1	Cl	Acetone (1 : 2)	92.5(7)	−1.6(5)	−1.6(5)
2	Bu^t	Acetone (1 : 1)	89.1(6)	−26.9(5)	−26.9(5)
3[a]	Cl	1,4-Dioxane (2 : 7)	101.4(6)	−2.0(7)	−8.5(7)
4[a]	Cl	1,3-Dioxolane (1 : 2)	94.2(7)	−10.9(5)	−10.9(5)
5[b]	Bu^t	Butyronitrile (1 : 1)	88.4(6)	−28.5(7)	−28.5(7)
6[b]	Cl	Cyclohexanone (1 : 2)	89.0(9)	−22.4(8)	−28.1(8)
7[b]	Cl	Cyclopentanol (1 : 2)	90.8(9)	−25.2(8)	−27.1(9)
8[b]	Br	DMF (1 : 2)	92(2)	−1(2)	−3(2)
9[c]	H		90.9(5)	−23.5(5)	−21.8(5)

[a] Ref. 11. [b] Ref. 6. [c] Ref. 5.

viewed along [001] is shown in Fig. 6. The acetone guest molecules are indicated with van der Waals radii and are located in constricted channels parallel to [001]. It is clear from a space filled diagram of the host with the guest omitted (Fig. 7) that these channels become as narrow as 1.7 Å. The host hydroxy hydrogen atom is disordered over two positions (each with 0.5 site occupancy) giving rise to 'flip-flop' hydrogen bonding. The host molecule is locked into conformation [with C(10A)–C(11A)–C(11A′)–C(10A′) = 89.1(6)°] *via* an intramolecular hydrogen bond [O(9A)–H(9A)···O(9A′) = 2.752(5) Å]. An intermolecular hydrogen bond exists between the guest molecule and host with O(9A)–H(9B)···O(3G) = 2.691(9) Å. Fig. 8 illustrates the two alternating hydrogen bonding motifs

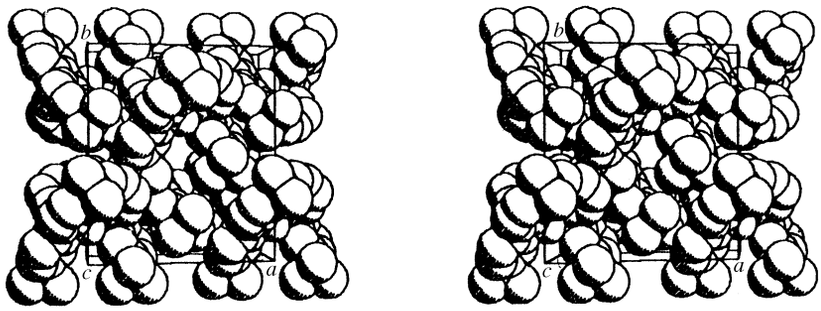

Fig. 7 Space filled diagram of the host network in compound **2** as viewed down [001]

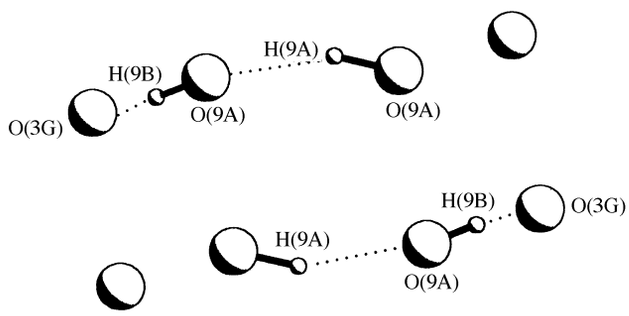

Fig. 8 Flip-flop hydrogen bonding observed in compound **2**

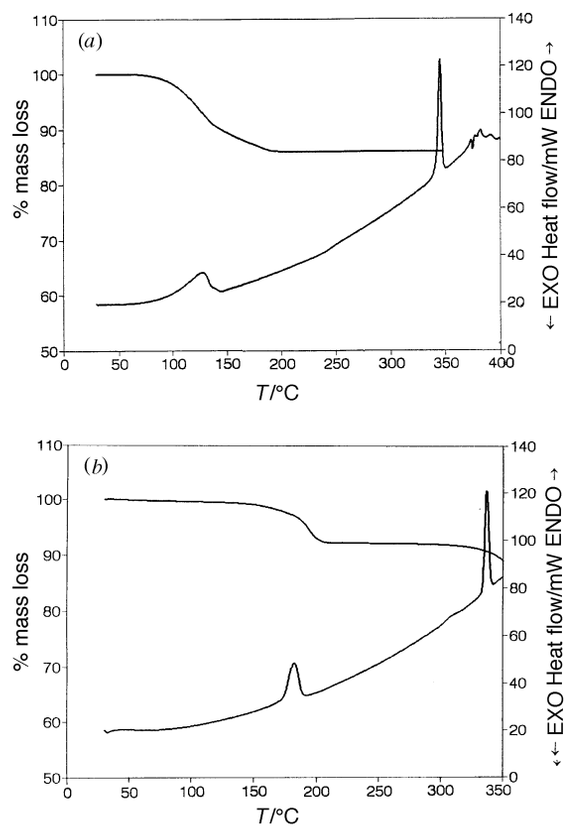

Fig. 9 (*a*) Thermograms showing the desolvation of compound **1**. (*b*) Thermograms showing the desolvation of compound **2**.

observed in the structure depending on the position of the guest molecule.

The conformation of the host molecules is governed by three torsion angles, τ_1, τ_2 and τ_3, indicated in Scheme 1. The two benzene rings in the central biphenyl are approximately at right angles, and Table 2 compares the torsion angle around the bond linking these rings, τ_1, and the other torsion angles for host molecules derived from similar structures.[6] Torsion angle τ_1 varies from 88.4–101.4°, while τ_2 and τ_3 span a wide range

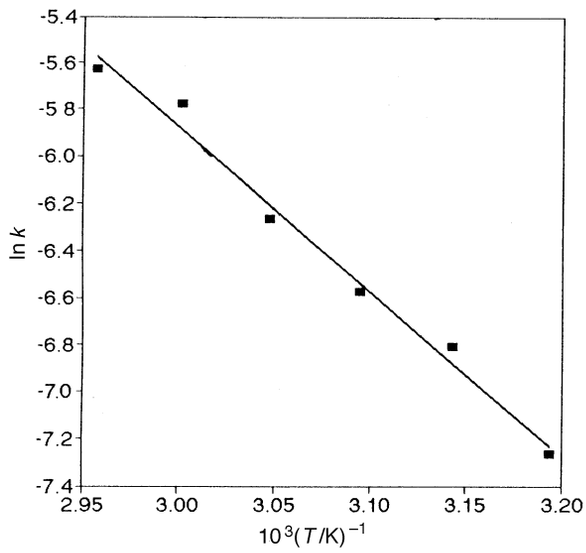

Fig. 10 Arrhenius plot for the desolvation of compound **1**

from −28.5 to −1°. The bond lengths and angles in the host molecules are in the accepted ranges for structures of this kind.[5,6,11]

Thermal analysis

The thermal analytical results are shown in Fig. 9(*a*) and (*b*). For compound **1** the guest loss reaction takes place in a single step, with a mass loss of 14%, corresponding to the loss of 2 acetone molecules. The DSC trace shows a diffuse endotherm, with an onset temperature of 80 °C, corresponding to the desolvation process. A sharp endotherm at 340 °C corresponds to the host melt. The host : guest ratio of 1 : 1 for compound **2** was confirmed by the TG experiment, showing a single mass loss step of 7.6%. This corresponds to a single sharp endotherm in the DSC trace at an onset temperature of 175 °C, followed by the melt at 334 °C. Compound **2** clearly desolvates at a much higher temperature than compound **1**.

Kinetics of desolvation

A series of mass loss *vs.* time curves were obtained for the isothermal desolvation of compound **1**, over a temperature range of 40–65 °C. The data were reduced to fractional reaction, α, *vs.* time curves. All these curves were deceleratory. Various appropriate kinetic models[14] were tested for linearity and the data were best fitted by the equation representing a three dimensional diffusion mechanism (D3) [eqn. (1)]. The plot of ln

$$[1 - (1 - \alpha)^{1/3}]^2 = kt. \quad (1)$$

k *vs.* $1/T$ is shown in Fig. 10, and yields an activation energy of 58(3) kJ mol^{-1} over an α-range of 0.05–0.90.

A series of isothermal TG experiments was carried out on compound **2** over a temperature range of 125–145 °C. Below 125 °C the reaction did not reach completion. The α *vs.* time

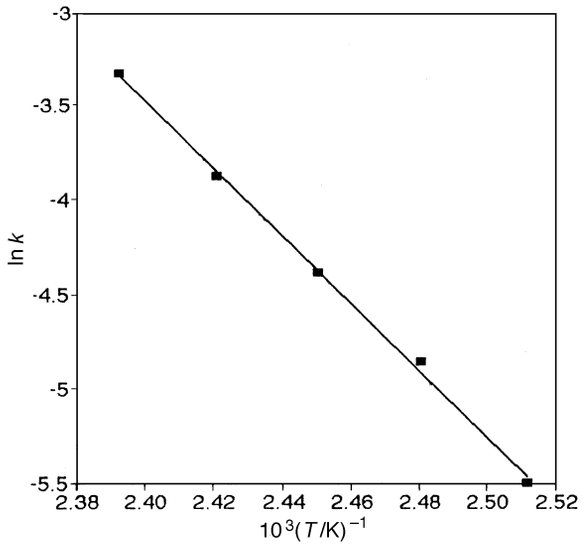

Fig. 11 Arrhenius plot for the desolvation of compound **2**

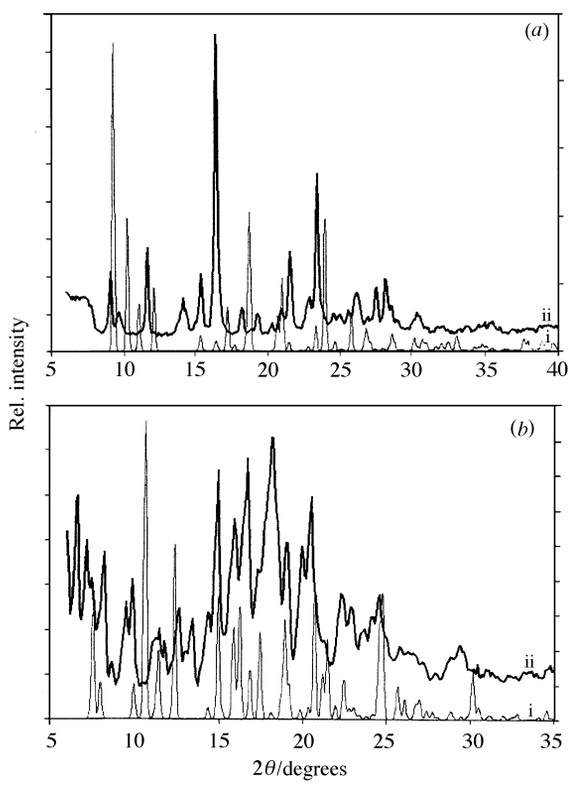

Fig. 12 (*a*) XRD patterns for compound **1** (i) calculated from the crystal structure and (ii) obtained experimentally after desolvation. (*b*) XRD patterns for compound **2** (i) calculated from the crystal structure and (ii) obtained experimentally after desolvation.

curves were deceleratory and were best described by the first-order (F1) kinetic model [eqn. (2)]. An activation energy of

$$-\ln (1 - \alpha) = kt \qquad (2)$$

147(4) kJ mol^{-1} was obtained for this reaction over an α-range of 0.05–0.95. A curve of ln k *vs.* 1/T is shown in Fig. 11.

X-Ray powder diffraction

The X-ray powder diffraction (XRD) patterns for compounds **1** and **2** were calculated from the atomic coordinates and Debye–Waller factors, obtained from the single crystal structure solution, using the program LAZYPULVERIX.[16] These patterns are compared with the experimentally obtained XRD patterns of the desolvated host compounds in Fig. 12(*a*) and (*b*), for compounds **1** and **2**, respectively.

IR spectroscopy

The hydrogen bond strengths were evaluated using IR spectroscopy. The O–H stretch was observed at 3420 cm^{-1} for compound **1** and at 3300 cm^{-1} for compound **2**. The free O–H stretch is usually observed as a sharp peak around 3500 cm^{-1}. The amount of O–H stretch wavenumber shift, has been correlated with the O···O distance, the smaller the distance, the larger the shift.[17] The observed shift in O–H stretching frequency is in agreement with the O···O distances described in the crystal structure solution.

Conclusions

The desolvation reaction [reaction (3)] is accompanied by a

$$\text{Host}\cdot(\text{acetone})_{n(s,\beta)} \longrightarrow \text{Host}_{(s,\alpha)} + n\cdot\text{acetone}_{(g)} \qquad (3)$$

phase change in the crystal structure. The solvated, β form is transformed to the non-porous α-phase. This was confirmed by X-ray powder diffraction. The α *vs.* time curves for the desolvation of both compounds are deceleratory. Compound **1** desolvates according to the three dimensional diffusion model. The rate of a diffusion-limited reaction is determined by the movement of reactants, or products, to or from, a reaction interface.[15] From the crystal structure it is clear that the guest molecules are located in channels running parallel to [010]. The reaction mechanism observed suggests that the diffusion of the guest is the rate-determining step in the desolvation of compound **1**. The model of unrestricted guest diffusion along the channels could explain the relatively low activation energy required for this reaction and the low temperature at which it takes place.

Compound **2** is much more stable than compound **1** and desolvates at a much higher temperature (significantly higher than the normal boiling point of acetone). This step is observed as a sharp endotherm in the DSC curve. The desolvation of compound **2** follows the F1 mechanism. There is no physical explanation for reactions based on order with respect to α, since concentration is not usually a meaningful term in solid state reactions.[14] The constricted channel structure however would imply that the gaseous decomposition product can escape only by severely disrupting the host framework. In addition we note that the host-to-guest hydrogen bonding is stronger in compound **2** than in compound **1**. A further possible explanation of the stability and higher activation energy observed for compound **2** lies in the fact that the host molecules are rendered rigid by an intramolecular hydrogen bond. This may also impede the phase transformation to the α form, which occurs upon desolvation. It is important to note that the change in phase cannot be accounted for in the kinetic models obtained, since the extent of reaction was measured as a function of the guest loss.

Acknowledgements

E. W. thanks the Deutsche Forschungsgemeinschaft and the Fonds der Chemischen Industrie for financial support.

References

1 M. R. Caira, A. Coetzee, L. R. Nassimbeni and F. Toda, *J. Chem. Res. (S)*, 1996, 280.
2 *Inclusion Compounds*, eds. J. L. Atwood, J. E. D. Davies and D. D. MacNicol, Academic Press, London, 1984, vols. 1–3; Oxford University Press, 1991, vol. 4.
3 F. Toda, in *Molecular Inclusion and Molecular Recognition-Clathrates I; Topics in current chemistry*, ed. E. Weber, Springer-Verlag, Berlin–Heidelberg–New York, 1987, vol. 140, p. 43.
4 S. A. Bourne, L. Johnson, C. Marais, L. R. Nassimbeni, E. Weber, K. Skobridis and F. Toda, *J. Chem. Soc., Perkin Trans. 2*, 1991, 1707.

5 L. J. Barbour, S. A. Bourne, M. R. Caira, L. R. Nassimbeni, E. Weber, K. Skobridis and A. Wierig, *Supramol. Chem.*, 1993, **1**, 331.
6 I. Csöregh, E. Weber, L. R. Nassimbeni, O. Gallardo, N. Dörpinghaus, A. Ertan and S. A. Bourne, *J. Chem. Soc., Perkin Trans. 2*, 1993, 1775.
7 D. R. Bond, M. R. Caira, G. A. Harvey, L. R. Nassimbeni and F. Toda, *Acta Crystallogr., Sect. B*, 1990, **46**, 771.
8 S. A. Bourne, L. R. Nassimbeni, M. L. Niven, E. Weber and A. Wierig, *J. Chem. Soc., Perkin Trans. 2*, 1994, 1215.
9 E. Weber, in *Kirk-Othmer Encyclopedia of Chemical Technology*, ed. J. I. Kroschwitz, Wiley, New York, 4th edn., 1995, vol. 14, p. 122.
10 L. J. Barbour, M. R. Caira, A. Coetzee and L. R. Nassimbeni, *J. Chem. Soc., Perkin Trans. 2*, 1995, 1345.
11 M. R. Caira, A. Coetzee, L. R. Nassimbeni, E. Weber and A. Wierig, *J. Chem. Soc., Perkin Trans. 2*, 1995, 281.
12 G. M. Sheldrick, SHELX-86, *Crystallographic Computing 3*, eds. G. M. Sheldrick, C. Kruger and R. Goddard, Oxford University Press, Oxford, 1985, p. 175.
13 G. M. Sheldrick, SHELX-93, *A Program for Crystal Structure Determination*, paper in preparation.
14 P. Schuster, G. Zundel and C. Sanderfy, *The Hydrogen Bond II, Structure and Spectroscopy*, North Holland Publishing Co., Amsterdam, 1976, 411.
15 M. E. Brown, D. Dollimore and A. K. Galwey, *Comprehensive Chemical Kinetics*, eds. C. H. Bamford and C. J. Tipper, Elsevier, Amsterdam, 1980, vol. 22, p. 220.
16 K. Yvon, W. Jeitschko and E. Parthé, *J. Appl. Cryst.*, 1977, **10**, 73.
17 N. B. Colthup, L. H. Daly and S. E. Wiberley, *Introduction to Infrared and Raman Spectroscopy*, Academic Press, San Diego, 3rd edn., 1990, pp. 210–211.

Paper 6/05502H
Received 6*th August* 1996
Accepted 7*th October* 1996